DOE/PC/92521--T69

FINAL TECHNICAL REPORT*
September 1, 1992 through August 31, 1993

Project Title: **BEHAVIOR OF SULFUR AND CHLORINE IN COAL DURING COMBUSTION AND BOILER CORROSION**

DE-FC22-92PC92521

Principal Investigator: C.-L. Chou, Illinois State Geological Survey (ISGS)

Other Investigators: K.C. Hackley, J. Cao, D.M. Moore, J. Xu, and R.R. Ruch, ISGS; W.-P. Pan, M.L. Upchurch, and H.B. Cao, Western Kentucky University

Project Manager: K.K. Ho, Illinois Clean Coal Institute

ABSTRACT

The goals of this project are to investigate the behavior of sulfur and chlorine during pyrolysis and combustion of Illinois coals, the chemistry and mineralogy of boiler deposits, the effects of combustion gases on boiler materials, and remedial measures to reduce the sulfur and chlorine compounds in combustion gases.

Replicate determinations of chlorine and sulfur evolution during coal pyrolysis-gas combustion were conducted using a pyrolysis apparatus in conjunction with a quadrupole gas analyzer. HCl is the only gaseous chlorine species measured in combustion gases. Pyrolysis of coal IBC-109 spiked with NaCl solution shows a strong peak of HCl evolution above 700°C. The absence of this peak during pyrolysis of Illinois coal indicates that little chlorine in Illinois coal occurs in the NaCl form. Evolution of sulfur during coal pyrolysis was studied; the sulfur evolution profile may be explained by the sulfur forms in coal.

To determine the fate of sulfur and chlorine during combustion, a set of six samples of boiler deposits from superheater and reheater tubes of an Illinois power plant was investigated. Scanning electron microscopy shows microscopic calcium sulfate droplets on cenospheres. Superheater deposits are high in mullite, hematite, and cristobalite, whereas a reheater deposit is enriched in anhydrite. The chlorine content is very low, indicating that most of the chlorine in the feed coal is lost as volatile HCl during the combustion process. The profiles of SO_2 released during combustion experiments at 825°C indicate that calcium hydroxide added to the coal has a significant effect on reducing the SO_2 vapors in combustion gases.

*U. S. DOE Patent Clearance is NOT required prior to the publication of this document.

EXECUTIVE SUMMARY

Any corrosion observed in a boiler is an elaborate combination of several factors, which include the amount of liquid sulfate on the superheater tube, the sulfur content of coal, the chlorine content of coal, the temperature of the superheater tube wall, and the chemical composition of the alloy (Bakker et al., 1990). The chlorine content of coal is not the only factor that causes boiler corrosion. An important purpose of this project is to better understand how these factors are related to superheater corrosion and ash deposition in coal-fired power plants. Our approaches include the determination of gaseous species of sulfur and chlorine in combustion gases and their release profiles, chemistry and mineralogy of boiler deposits, and effects of combustion gases on boiler material.

Knowledge about the forms of chlorine in coal and the manner it is released during pyrolysis and combustion is helpful in understanding any role that chlorine has in boiler corrosion. New experiments of determining HCl release profiles were conducted using a temperature-programmed pyrolysis and gas combustion apparatus with a quadrupole gas analyzer (QGA). Chou (1991) suggested that there are two forms of chlorine in Illinois coals: most of the chlorine occurs as chloride ions adsorbed on inner walls of the pores, the rest of the chlorine is in the form of Na^+Cl^- dissolved in coal moisture in large pores and cracks. To determine the behavior of NaCl during coal pyrolysis, pyrolysis of Illinois coal IBC-109 spiked with NaCl solution showed a strong peak of HCl evolution starting at 700°C and extending over 850°C. The absence of this peak in the profiles of coal indicates that only a small fraction of the chlorine, in the coals tested, occurs as NaCl.

The mineralogy of boiler deposits was studied by X-ray diffraction analysis. Several procedures for sample preparation (random powder bulk pack, oriented slides, and water washing to remove anhydrite) were developed. Minerals in superheater and reheater deposits are mainly mullite ($3Al_2O_3 \cdot 2SiO_2$), quartz (SiO_2), cristobalite (high-temperature silica), anhydrite (calcium sulfate, $CaSO_4$), hematite (iron oxide, Fe_2O_3), feldspar [$(Na,K)AlSi_3O_8$], and sodium iron trisulfate [$Na_3Fe(SO_4)_3$]. Minerals in furnace wall and economizer are: magnetite (Fe_3O_4), cristobalite, hematite, plagioclase, and sodium iron trisulfate.

SEM and petrographic examination revealed considerable details of boiler deposit formation. Molten droplets of hematite are coated with anhydrite rim, as a result of sequential melting and condensation. XRF determination of 27 major, minor, and trace elements shows considerable compositional variations. Sodium and chlorine in the deposits were determined by neutron activation analysis. Chlorine is highly depleted in superheater and reheater samples (<40 $\mu g/g$), indicating HCl

was lost to the atmosphere during combustion. Na and K are enriched in ash deposits. For instance, Na/Al ratio in the deposits is 1.5 - 3 times that in the feed coal.

Laboratory experiments were conducted to study the effects of composite gases (N_2, CO_2, O_2, SO_2 and HCl) on six metals at 600°C and 200°C, and in the presence of moisture at 100°C. Similar tests were conducted with a composite gas containing no HCl at 600°C and 200°C. The results allow us to assess the factors that control the corrosion of superheater and reheater tubes: boiler materials, temperature, concentration of HCl in combustion gases, and chloride condensate on metal surfaces. It should be emphasized that the conditions of laboratory tests are not identical to utility and industrial boilers, because ash is not involved in the laboratory experiments and there is no deposits formed on the metal coupons. Because of these limitations, the results of laboratory tests can not be extrapolated to boiler conditions. Further boiler tests are needed to evaluated the effects of chlorine on boiler corrosion. The current understanding of the effects of chlorine on superheater corrosion in utility boilers is provided by a recent EPRI report by E.P. Latham and Chamberlain (1992, EPRI TR-101729).

OBJECTIVES

The purpose of the project is to study the behavior of sulfur and chlorine during coal pyrolysis and combustion, mineralogical and chemical compositions of boiler deposits, effects of HCl and SO_2 in combustion gases on boiler metals, and remedial measures to reduce the HCl concentration in boiler gases. The specific goals of the project are to:

- Develop methods to identify sulfur and chlorine species in pyrolysis and combustion gases
- Determine gas evolution profiles for sulfur and chlorine during temperature-programmed pyrolysis-gas combustion, and during thermogravimetry
- Determine sulfur species in combustion gases under oxidizing and reducing conditions
- Determine mineralogical and chemical compositions of superheater and reheater deposits
- Laboratory tests to determine the effects of composite gases containing HCl and SO_2 on metals of different Cr contents
- Evaluate the use of additives in reducing sulfur and chlorine concentrations in combustion gases

INTRODUCTION AND BACKGROUND

Evolution of volatile chlorine species during coal pyrolysis in a nitrogen atmosphere at a heating rate of 20°C/min was investigated. During the previous year we developed two techniques for determination of chlorine gaseous species in combustion gases (Chou et al., 1992a). HCl was the only gaseous chlorine species identified in combustion gases. The HCl release profile for Illinois coal IBC-109 (0.42% chlorine on dry basins) showed a broad peak between 250°C and 600°C with a maximum at 445°C. During this year we made systematic determination of SO_2 and HCl evolution during coal combustion using different weights of IBC-109 and using Illinois Basin coals of different chlorine contents. To study the behavior of NaCl component of the chlorine in coal during pyrolysis, experiments on coal combined with NaCl powder and coal spiked with NaCl solution were conducted.

Chemical and mineralogical compositions of deposits from the

superheater and reheater in utility boilers are important because corrosion loss of metal tubes may be related to the amounts of the alkali sulfate in boiler tube deposits. Furthermore, the chlorine content in boiler deposits provides information about the behavior and fate of chlorine in the boiler. Six boiler deposits from superheater and reheater tubes in a utility boiler have been examined. Each deposit is separated into inner and outer portions and analyzed for mineralogical composition by X-ray diffraction, microstructure by scanning electron microscopy, and major, minor, and trace elements by X-ray fluorescence spectrometry and neutron activation analysis. There is considerable variation of chemical compositions among the twelve samples. For example, the CaO content varies from 3.55% to 20.04%, and the SO_3 content from 0.35% to 20.95%, indicating considerable chemical fractionation of ash and volatiles during coal combustion. The chlorine content in the samples is very low. Apparently most of the chlorine is lost during coal combustion because of its high volatility. This is an argument against the hypothesis that chlorine takes part in corrosion of the high-temperature portion of a boiler. Considerable effort was made in developing sample preparation procedures for X-ray diffraction analysis for precise identification of minerals. We have also determined the quantity of mineral phases in the boiler deposits based on reference intensity ratios of the minerals.

To study of the effects of composite gases on boiler materials, corrosion experiments were conducted on six metals exposed to a composite gas containing various amount of HCl and at 600°C and 200°C, and at 100°C with moisture for 400 hours. The results allow us to evaluate the factors affecting the superheater corrosion: materials (Cr content), temperature and combustion gas composition.

EXPERIMENTAL PROCEDURES

Experimental setup for temperature-programmed coal pyrolysis/gas combustion coupled with a QGA.

The experimental procedures were described previously (Chou et al., 1992). Major components of the experimental setup include a quartz tube reactor, a gas flow controller, two tube furnaces, a programmable temperature controller, a Dycor QGA, and a microcomputer. The quartz tube reactor consists of two consecutive chambers separated by a small orifice. Samples of coal are heated from ambient temperature to 800°C at a rate of 20°C/min in the pyrolysis chamber under a controlled atmosphere of nitrogen. The volatile products are carried with the nitrogen flow to the second chamber, which is

maintained at 850°C under a constant flow of oxygen. The gases flowing into the second chamber from the pyrolysis chamber are combusted. The combustion gases are sampled through a capillary tube and analyzed with a QGA. The gaseous species are identified based on their mass numbers.

Replicate analyses of HCl and SO_2 evolution from coal IBC-109 during pyrolysis were conducted using different sample weights of coal IBC-109. Four coal samples with different chlorine contents were studied.

Boiler deposits

Six samples of boiler deposits were collected from the final superheater and reheater areas of the Unit 5 boiler, Wood River Power Station, Illinois Power Company. Samples WR5-1, -2, -3, -5, and -6 are from the superheater area, and sample WR5-4 from the reheater area. It is a Combustion Engineering tangential-fired, pulverized coal boiler operating at 1,050°F main steam temperature and 1000°F reheat steam temperature. A diagram of the boiler with sample locations was included in a previous report (Figure 1 in Chou et al., 1992b).

Each of the six samples was examined in the laboratory and separated into inner (comparatively close to the tube surface) and outer portions, with the exception of sample WR5-4 and WR5-6. The inner portion is generally reddish and loosely aggregated, often friable, whereas the outer layer is brownish and relatively compact and firm.

Sample WR5-4 consists of a compact piece of brownish and reddish segments from the outer portion (2-3 cm thick). The brown and red portions were separated for analysis.

Sample WR5-6 consists of a brownish, firm framework filled by brownish grey powder. The grey powder (loosely compacted) was separated and makes up WR5-6b (XRD #3463L) (Table 1).

Separate aliquots of the 12 samples were pulverized to 100 mesh (about 150 μm) powder using a ball mill and analyzed by X-ray diffraction analysis for mineralogical composition and by X-ray fluorescence spectrometry and neutron activation analysis for chemical compositions. Part of the SEM examination and chemical compositions were reported earlier (Chou et al., 1993a). The samples and laboratory numbers are listed in Table 1.

<u>X-ray diffraction analysis using random powder bulk packs and other sample preparation methods</u>

All 12 samples were first analyzed as random powder bulk packs

by XRD using Cu K-alpha radiation. About 3.5 g of a powder sample was weighted out and wet-ground in propanol for six minutes in a micronizing mill to <5 μm. The sample was then poured into a beaker and dried in an oven at 75°C. Upon drying, the powder was packed in a side-loading sample holder ready for X-ray scanning. The XRD patterns of the twelve samples of boiler deposits were determined this way.

To eliminate some overlapping peaks on the XRD patterns, we selectively dissolved some minerals. Of the 12 samples, 4 were chosen to be examined as oriented slides and re-examined in random powder bulk pack after a water washing process to remove anhydrite.

Table 1. Samples

Sample	Description	Chem. Anal. No.	XRD Lab No.
Superheater samples			
WR5 -1a	Outer portion	C32825	3463A
-1b	Inner portion	C32826	3463B
WR5 -2a	Outer portion	C32827	3463C
-2b	Inner portion	C32828	3463D
WR5 -3a	Outer portion	C32829	3463E
-3b	Inner portion	C32830	3463F
WR5 -5a	Outer portion	C32833	3463I
-5b	Inner portion	C32834	3463J
WR5 -6a	Outer, brown	C32835	3463K
-6b	Inner, gray	C32836	3463L
Reheater sample			
WR5 -4a	Outer portion, brown	C32831	3463G
-4b	Outer portion, red	C32832	3463H

Oriented slides

In order to distinguish layered silicates and/or minerals with well developed cleavage from other mineral phases, samples WR5-1a (3463A), -3b (3463F), -4b (3463H), and -6b (3463L) were selected to make oriented slides with <1 μm and <4 μm particles, respectively. These four samples represent the full range of variation found in the set of 12. The samples were prepared according to the following procedures: put about 5 g powdered sample (<150 μm particles) in 100 ml distilled water; disperse ultrasonically for 1 minute; extract the fluid in the top 1 cm after the sample has settled for 12 minutes for <4 μm size fraction and 3 hours 10 minutes for <1 μm size fraction, respectively; put the fluid on a glass slide with an eye dropper, then let the slides dry at room temperature. The dried fine-particle aggregate will be the oriented sample. The XRD pattern of the oriented slide is dominated by gypsum peaks, indicating that anhydrite was dissolved in water and re-crystallized on the slide as gypsum. To observe other minerals, further steps (water washing) were applied to these samples to remove anhydrite.

Water washing to remove anhydrite

The water washing procedures are as follows: transfer about 3 g of powdered sample (<5 μm) to a beaker (700 mL) and fill with distilled water, centrifuge the content to settle the undissolved material, pour off the clear solution, refill with distilled water, and repeat these steps 3 times. Monitoring slides were made from the clear solution to check the wash effect. The first two wash solutions crystallized gypsum on the slides, but the third was clear and its XRD pattern showed only the background typical of the glass of which the slide was made. This indicates that anhydrite is removed by three washing steps. After the water wash, the sample was re-examined as a random powder bulk pack. The washing procedure simplified the XRD patterns for the random powder bulk packs allowing unambiguous identification of hematite and feldspar, and, also, confirmed the anhydrite interpretation.

Sample WR5-4b (3463H) has high CaO (20.04%) and SO_3 (20.95%) contents. The unwashed sample shows strong anhydrite peaks, which are absent in the washed sample (Figure 4a in Chou et al., 1993b).

Sample WR5-6b (3463L) has high Fe_2O_3 (12.1%) and Al_2O_3 (23.03%) contents. The washed sample shows clearly hematite, mullite, quartz and cristobalite peaks (Figure 4b in Chou et al., 1993b).

The reference intensity ratios used in this study are given in

Table 2.

Table 2. Reference intensity ratios (RIR's) of the minerals

Mineral	Peak used °2θ/Å	RIR
Quartz	20.85/4.26	1.00
Quartz	50.1/1.82	1.57
Anhydrite	25.5/3.49	0.44
Cristobalite	21.5/4.05	0.22
Feldspar	27.5-28.0/3.24-3.18	0.39
Hematite	35.6/2.52	2.0
Mullite	16.4/5.39	3.00
Nepheline	23.1/3.85	0.60
X-Ray Amorphous	17-35/5.2-2.5	0.08

Effect of composite gases on metals at various temperatures

The purpose of these experiments is to define a set of parameters that outline corrosion effects on metals using simulated combustion gases. Three variables are considered: HCl concentration, length of exposure time, and temperature under isothermal conditions.

Evaluation of corrosion for any metal is dependent on the length of a particular experimental run. The experiments are run at three different temperatures (100°C, 200°C, and 600°C). The temperature of 600°C is chosen because it simulates a common superheater temperature. The 100°C temperature is chosen to determine the interaction of water, as it condenses or evaporates, with metals on the corrosion rate. Therefore, for the 100°C run, water vapor is introduced to the samples by passing nitrogen gas first through a water bath then to the furnace.

The rate of corrosion is evaluated by weight gain or loss per unit of time. The furnace design is shown in a previous report (Figure 2 of Chou et al., 1992b). Experiments were conducted using three composite gases with 0.2%, 0.01%, and 0% HCl. A 0.01% HCl concentration in combustion gas is equivalent to burning coal with 0.125% chlorine.

RESULTS AND DISCUSSION

SO_2 evolution during coal pyrolysis/gas combustion

Replicate pyrolysis/gas combustion experiments were conducted on three different sample weights (0.25 g, 0.50 g, and 0.75 g) of coal IBC-109. Figure 1 showed that the partial pressure of SO_2 is proportional to the sample weight (or the amount of sulfur). This demonstrates that this method of determining sulfur evolution profiles is accurate and correlates well with quantitative measurements.

HCl evolution using a pyrolysis/gas combustion apparatus with quadrupole gas analyzer

Figure 2 shows HCl evolution profiles during replicate coal pyrolysis/gas combustion with different sample weights of coal IBC-109. Five HCl release profiles are determined by quadrupole gas analysis (mass number 36) using increasing amounts (from 0.25 g to 1.25 g) of high-chlorine coal IBC-109. The HCl gas evolution from the coal begins at approximately 300°C (±10°C). The maximum rate of HCl release occurs at approximately 445°C; at 600°C the release of HCl is nearly complete. The relation between the intensity of the HCl profile and the amount of coal (in turn the amount of chlorine) is clearly demonstrated.

Four Illinois coals of decreasing chlorine content from 0.42% (IBC-109), 0.18% (IBC-103), 0.10% (IBC-101), to 0.02% (IBC-102) (on dry basis) were studied. HCl evolution profiles of these four samples are obtained (Figure 3), showing that the HCl partial pressure decreases with decreasing chlorine concentration in coal. The profile for coal IBC-102 is close to the background level because of its low chlorine content. Thus, this method for determining HCl evolution during pyrolysis is accurate and correlates well with quantitative measurements.

Pyrolysis of a mixture of coal and NaCl

To determine the behavior of NaCl during coal pyrolysis, pyrolysis tests on mixtures of coal sample plus NaCl were conducted. Pyrolysis of a mixture of coal IBC-102 (sample #102a, 0.62 g) and NaCl (24.6 mg) generates a HCl evolution profile with peaks between 260°C and 600°C and a stronger peak from 700°C and above (run EL92083b) (Figure 5 in Chou et al., 1993a). Figure 4 shows the results when coal IBC-109 was spiked with NaCl solution (25 mg NaCl), and the sample was dried and subjected to a pyrolysis run. The results showed a new HCl evolution peak starting at 700°C and extending over 850°C, probably as a result of the reaction of NaCl with

organic matter. This profile is different from those obtained by pyrolysis of Illinois coals without adding NaCl (absence of a +700°C peak), suggesting that the Illinois coals contain only insignificant amount of NaCl.

Boiler deposits: X-ray diffraction study

Mineral phases in the boiler deposit samples were identified by X-ray diffraction (XRD) technique. The XRD patterns of twelve samples (XRD analysis No. 3463A-L) were reported by Chou et al. (1993a). Most samples seem to contain more than six phases (quartz, cristobalite, mullite, anhydrite, hematite, and feldspar) and some x-ray amorphous (XRA) material.

Abundances of the mineral phases vary from sample to sample as indicated by the relative intensity of XRD peaks. The best estimate of mineral phases present in each sample is tabulated in Table 3. Samples A through F are rather similar, but samples G through L are different from one another and different from A through F. Mullite, quartz, and anhydrite are the most common phases. Feldspar or a feldspar-like phase is present. It is predominantly plagioclase but varies somewhat in composition from sample to sample. For example, it is an albite-like phase in some samples and a bytownite-like phase in others. A shoulder on the low angle side of the plagioclase peak at ~27.9°2θ suggests the presence of K-feldspar. We report all feldspars as one phase (Table 3). The peaks of hematite and mullite have an almost perfect match except for a hematite peak at 24.14° and one at 35.6°2θ and a mullite peak at 16.4°2θ. Hematite may vary in particle size because the 24.14° peak in sample F, tentatively identified as a hematite peak, is quite broad. The 33.12° position is quite popular for the assemblage of phases in these samples. The strongest hematite peak is here; a mullite peak with I/I = 40 is here; an anhydrite peak with I/I = 35 is here; several varieties of apatite have their strongest peak here; and several materials that are problematically present would have a peak here. Nepheline, $Na_4Al_4Si_4O_{16}$ is present in the reheater sample, WR5-4b or H, also the sample with the maximum amount of XRA material. We make this identification knowing full well that it is an axiom of igneous petrology that quartz and nepheline never occur together. Perhaps we can rationalize the co-existence of these two minerals by saying that this is not an equilibrium assemblage.

We have used samples A, F, H, and L as a subset of the whole sample set. Having examined them, we can make some qualitative assessments with confidence: reheater sample H has the maximum amount of anhydrite; sample L contains the maximum amount of cristobalite, the minimum amount of XRA material,

Table 3. Abundances of mineral phases in twelve boiler deposit samples#

Sample	Quartz	Cristobalite	Mullite	Feldspar	Nepheline	Hematite	Anhydrite	XRA*
Superheater deposits								
A, WR5-1a	14	2	20	15	0	26	7	16
B, WR5-1b	19	3	19	14	0	20	6	19
C, WR5-2a	14	2	18	17	0	22	7	20
D, WR5,2b	17	1	22	11	0	18	6	25
E, WR5-3a	12	2	20	18	0	25	5	18
F, WR5-3b	18	4	18	12	0	21	8	19
I, WR5-5a	17	2	18	18	0	21	6	18
J, WR5-5b	21	3	19	14	0	16	8	19
K, WR5-6a	4	8	8	7	0	34	29	10
L, WR5-6b	7	20	24	0	0	34	9	6
Reheater deposits								
G, WR5-4a	9	2	16	19	0	19	14	21
H, WR5-4b	13	0	0	5	1	21	51	9

#Mineral phases total 100%
*X-ray amorphous phase

and feldspar seems absent. We have searched for a phosphorus(P)-bearing phase in sample G because it contains 1.55% P (Table 4), we can't find it. With so many peaks, identification of phases present in small amounts becomes difficult. For example, clinopyroxene has been reported in low-temperature ashes (LTA's). In the XRD tracings of our samples, all eight of the most intense lines coincide with those of the more common phases present. For the same reason, two hydrated phases, alunite [$(K,Na)Al_3(SO_4)_2(OH)_6$] and collinsite [$Ca_2Mg(PO_4)2{\cdot}2H_2O$] might be present. Collinsite is another mineral with its strongest line at 33.1°2θ. Alunite could be present in sample F but the two strongest peaks are so small that they could also be taken for part of the background. If phases with OH's or H_2O are present, they would have to have formed after removal from the boiler. Complex alkali-metal sulfate phases were deliberately looked for but were not present.

Samples F, H, and L were carefully checked for six different varieties of apatite, for the Ti minerals anatase, brookite, ilmenite, and rutile, and for $MgAl_2O_4$. Only ilmenite is a faint possibility and that only for two small peaks in sample L.

It should be emphasized that the values given in Table 3 do not represent quantitative analyses. We can claim internal consistency. The relative order of abundance should be valid but the values given represent too many approximations, too many ignored complexities, and too complex of a system for them to have high accuracy. The values for X-ray amorphous (XRA) material, especially, represent estimates based partly on numbers from the XRD tracings, partly from inspection of thin sections, and partly an intuitive guess about how much amorphous material ought to be present. In spite of the impressive linearity shown in Figures 5a and 5b, the RIRs used (Table 2) are approximations. For example, because hematite absorbs radiation significantly more than quartz, for our laboratory mixture of quartz and hematite, the intensity of quartz for concentrations of more than 25% hematite drops off in a non-linear fashion. I suspect our measures of hematite may be too low.

Boiler deposits: petrographic observations

The six samples of boiler deposits (WR5-1 to WR5-6) were impregnated with blue epoxy and made into thin sections. Pieces were selected so that material (or scale) from inner portion close to boiler pipes and outer portion of material away from the pipes and closest to the stream of flue gases are represented in the same thin section. Samples WR5-4a and WR5-4b were made into separate thin sections because of the

distinctive color and texture difference in the outer portion. Quartz, hematite, cristobalite (after having been determined by XRD), anhydrite, and mullite are identified under the microscope. Samples WR5-4a, -4b, and -6 were analyzed by SEM/EDX to confirm XRD and microscopic identifications. Characteristic texture indicates two origins for the minerals: either crystallization from a melt or unaltered from raw coal. Quartz often occurs as dispersed grains; other minerals commonly form aggregates or droplets. Individual minerals are described as follows.

Quartz (SiO_2) is present as dispersed grains in the ash deposits, mostly in subhedral shape, clean, and of silt-size. It constitutes as about 5-20% by volume. Some quartz grains have irregular cracks, perhaps from changing from α-quartz in ambient temperature to β-quartz upon heating during combustion.

Cristobalite (SiO_2) is found only in sample WR5-6, as determined by XRD. Some quartz grains in this sample occur as partly quartz and partly cristobalite, probably due to transformation from quartz to cristobalite upon heating in the boiler.

Hematite (Fe_2O_3) is easily identified in thin sections because it is opaque and brownish in reflected light. It also is clearly identified from XRD (Chou, et al., 1993a). Hematite occurs mainly in two forms: as droplets (Figure 6) and in strips. Droplets are the most common form of hematite with sizes of several tens of micrometers in diameter. The reheater sample WR5-4a, in richest in hematite (about 25% by volume). A few of the droplets are empty hematite shells. The spherical shape of the hematite droplets suggests that they solidified from molten melt. Almost all of the droplets are coated by an anhydrite rim (Figure 6). Hematite also occurs as coatings on the outer rim of the samples; the hematite strips within the sample appear to be "buried outer edges". Hematite was also found in mixed aggregates.

Anhydrite ($CaSO_4$) is present mainly as a coating on the droplets of primarily hematite, though large anhydrite crystals were found as pore-filling. Radiative fibrous texture is clear in the anhydrite coatings. An EDX spectrum of an anhydrite rim showed strong Ca and S peaks. Anhydrite also coats some quartz grains and is present in mixed aggregates.

Mullite ($Al_6Si_2O_{13}$) occurs as grey dusty aggregates under the microscope. Under SEM the bubble shape of mullite is observed, indicating its formation from a melt. The optical properties of mullite was difficult to determine because of its small

particle sizes. An EDX spectrum with silicon and aluminum peaks helped in its identification. Mullite is believed to have formed mainly from clay minerals in coal. Calcium and iron also present in the mullite aggregate, which may be derived from decomposition of pyrite and calcite. Mullite also occurs as droplets of mixed crystal aggregates.

Material that appears amorphous to X-rays (XRA) is present. However, its presence is difficult to measure or detect. Its presence is most clearly expressed by a rising the normal background on XRD tracings. Correspondingly, we estimated the amount present by measuring "excess" background between 17 and 35°2θ (CuKα radiation) (see Table 2).

Though every mineral is present in its own more or less distinct form, aggregates, some in the form of droplets are apparently mixtures of hematite, mullite, anhydrite, and amorphous material. The droplet usually has hematite-like optical features under the microscope. SEM/EDX analyses support the conclusion that some of the droplets are aggregates. A typical EDX spectrum of this kind of droplet shows complex composition (with Mg, Al, Si, S, Ca, Ti, and Fe peaks). Mixed aggregates make up a major portion of the sample.

Chemical composition of boiler deposits

The chemical compositions determined by X-ray fluorescence and neutron activation analysis are listed in Table 4. The major constituents in the deposits (>0.5%) are SiO_2, Al_2O_3, Fe_2O_3, CaO, MgO, K_2O, Na_2O, TiO_2, P_2O_5, and SO_3. The Al_2O_3 content is fairly uniform in mostly samples from 22.5% - 24.5%, except sample WR5-6a with 20.11% Al_2O_3 and WR5-4b with 10.84% Al_2O_3. Sample WR5-6a has high Fe_2O_3, CaO, Na_2O, and SO_3, indicating a possible high content of calcium sulfate; sample WR5-4b has high CaO and SO_3 contents.

Eight out of twelve samples have a SiO_2 content between 57% and 62%; the remaining four samples (WR5-6a,b and WR5-4a,b) have a lower SiO_2 content (30.4% - 51.4%). Samples WR5-6a,b are high in Fe_2O_3, SO_3 and alkalis. Samples WR5-4a,b are brown and red portions from the same piece of deposit. The brown sample WR5-4a is relatively high in CaO, MgO, Na_2O, TiO_2, P_2O_5, SO_3, and a high loss of ignition (volatile component). The red sample WR5-4b is rather unique in having low Al_2O_3 (10.8%) and K_2O, but high in CaO (20.0%), MgO, Na_2O, and SO_3 (about 21%), indicating an appreciable amount of hydrated calcium sulfate.

Table 4. Chemical compositions of ash deposits from superheater and reheater of a boiler determined by XRF and NAA (for Na and Cl only) (on dry basis except H_2O)

	Superheater deposits					
	WR5-1a (C32825)	WR5-1b (C32826)	WR5-2a (C32827)	WR5-2b (C32828)	WR5-3a (C32829)	WR5-3b (C32830)
Major and minor constituents (in %)						
SiO_2	60.36	62.08	58.49	59.64	57.89	60.75
Al_2O_3	22.94	22.46	23.51	23.37	23.50	22.47
Fe_2O_3	3.48	2.77	3.45	4.02	3.42	2.89
CaO	4.90	4.53	5.07	4.04	5.71	4.61
MgO	1.67	1.56	1.76	1.46	1.92	1.58
K_2O	1.16	1.11	1.21	1.33	1.13	1.10
Na_2O (XRF)	1.18	1.26	1.24	1.15	1.27	1.24
(INAA)	1.18	1.21	1.18	1.13	1.21	1.23
TiO_2	0.79	0.71	0.86	0.90	0.87	0.74
P_2O_5	0.72	0.46	0.90	0.61	0.99	0.65
MnO	0.02	0.01	0.01	0.02	0.02	0.01
SrO	0.20	0.19	0.22	0.17	0.24	0.20
BaO	0.39	0.37	0.42	0.35	0.45	0.40
SO_3	0.57	0.55	0.56	0.56	0.37	0.55
LOI*	1.26	1.49	1.75	1.92	1.59	2.33
Total**	99.64	99.55	99.45	99.54	99.37	99.52
H_2O	0.02	0.03	0.04	0.06	0.04	0.03

*At 1000°C
**XRF Na_2O value used

Table 4, continued

	Superheater deposits					
	WR5-1a (C32825)	WR5-1b (C32826)	WR5-2a (C32827)	WR5-2b (C32828)	WR5-3a (C32829)	WR5-3b (C32830)
Trace elements (in ppm)						
Cl(INAA)	<15	<15	<15	37	<15	<30
V	87	70	101	116	103	73
Cr	100	33	149	93	141	40
Co	31	28	32	36	29	26
Ni	41	26	45	53	41	27
Cu	65	36	83	72	80	42
Zn	124	36	186	129	195	48
Rb	42	37	46	53	42	37
Zr	364	350	370	349	386	357
Nb	21	19	26	23	26	20
Mo	2	2	4	4	4	3
Cd	nd	nd	1	nd	nd	nd
Sn	1	1	3	1	4	1
Pb	60	43	95	80	109	51

nd: not detected.

Table 4, continued

	Superheater deposits				Reheater deposits	
	WR5-5a (C32833)	WR5-5b (C32834)	WR5-6a (C32835)	WR5-6b (C32836)	WR5-4a (C32831)	WR5-4b (C32832)
Major and minor constituents (in %)						
SiO_2	58.97	60.24	39.96	45.43	51.42	30.40
Al_2O_3	23.40	23.04	20.11	23.03	24.53	10.84
Fe_2O_3	3.34	3.11	11.28	12.10	3.84	4.99
CaO	5.37	4.61	9.00	3.55	6.58	20.04
MgO	1.84	1.60	1.96	0.94	2.12	3.79
K_2O	1.13	1.12	1.84	1.68	1.13	0.43
Na_2O (XRF)	1.24	1.28	1.66	1.44	1.59	1.66
(INAA)	1.26	1.24	1.53	1.24	1.53	1.57
TiO_2	0.84	0.78	1.33	1.40	1.01	0.96
P_2O_5	0.90	0.71	0.61	0.40	1.55	0.45
MnO	0.02	0.01	0.05	0.03	0.01	0.02
SrO	0.23	0.20	0.14	0.07	0.27	0.23
BaO	0.43	0.39	0.18	0.06	0.51	0.45
SO_3	0.35	0.60	6.99	3.22	1.23	20.95
LOI*	1.42	1.79	4.42	6.17	3.58	4.43
Total**	99.48	99.48	99.53	99.52	99.37	99.64
H_2O	0.01	0.06	0.21	0.29	0.29	1.31

Table 4, continued

	Superheater deposits				Reheater deposits	
	WR5-5a (C32833)	WR5-5b (C32834)	WR5-6a (C32835)	WR5-6b (C32836)	WR5-4a (C32831)	WR5-4b (C32832)
Trace elements (in ppm)						
Cl(INAA)	<25	<40	<35	<45	<30	<45
V	87	78	308	292	129	140
Cr	101	41	783	335	155	136
Co	29	29	101	77	38	44
Ni	39	32	307	234	49	59
Cu	68	45	261	226	108	145
Zn	156	56	1425	943	243	364
Rb	40	39	108	105	43	23
Zr	373	360	291	260	369	260
Nb	24	22	33	32	33	18
Mo	4	2	13	12	8	16
Cd	nd	nd	7	5	2	11
Sn	1	2	11	6	7	nd
Pb	80	54	195	332	154	69

The chlorine content in the samples is very low. One sample (WR5-2b) contains 37 ppm chlorine. The others have a chlorine content below the detection limit (between 15 and 45 ppm). It appears that chlorine was lost during coal combustion. The chlorine in Illinois coal occurs as chloride ions adsorbed on the organic matter (Chou, 1991) and is highly volatile. Most of the sodium is not associated with chlorine and is largely retained in ash deposits.

Effects of composite gases with 0.2%, 0.01%, and 0% HCl on corrosion of metals

Six metals listed below were selected for tests:

AISI ID	Composition
C1010	8-13% C, 0.3-0.6% Mn
C1018	15-20% C, 0.6-0.9% Mn
T11	1.25% Cr, 0.5% Mo
T22	2.25% Cr, 1% Mo
310SS	25% Cr, 21% Ni
Alloy 800	21% Cr, 31% Ni

We previously reported the experiments with a composite gas containing 0.2% HCl (0.2% HCl, 0.2% SO_2, 4.0% O_2, 14.0% CO_2, and 81.6% N_2) on six metals (Chou et al., 1993b). Experiments were conducted at three different temperatures: 600°C, 200°C, and 100°C for 400 hours. At 600°C, three metals T11, T22, and C1010 have the greatest weight loss, metal C1010 has a less amount of weight loss, and high-Cr Alloy 800 and 310SS show no weight loss. The results indicate the material effect reflecting that chromium is an inhibitor of corrosion. At 200°C under otherwise similar conditions, no significant corrosion is observed. Different degrees of corrosion between 600°C and 200°C indicate a strong temperature effect on metal corrosion. The third set of experiments was conducted at 100°C and with the addition of water vapor. The Cr-Ni alloys show essentially no weight loss. The other four metals (T11, C1010, T22, and C1018) show different degrees of weight loss and the amounts of weight loss are smaller than those in the case of 600°C. Also during the experiments at 100°C, the weight loss occurs after the metals were exposed to the damp gas for 150 hours. In contrast, the weight loss starts at the beginning the run in the case of the 600°C test. The experiments are described in detail by Chou et al. (1993a,b). The rate of

weight loss was studied by regression analysis of the experimental results, and the relation between weight loss and corrosion rate and time was obtained (Chou et al., 1993b).

Experiments with a composite gas containing no HCl on six metals were reported by Chou et al. (1993b). The composite gas was composed of 0.2% SO_2, 4.0% O_2, 14.0% CO_2, and 81.8% N_2. At 600°C, metal T22 is the only metal showing significant weight loss (27% at the end of the 400 hour run). Metal T11 shows significant weight gain, 25% at the end of the run, indicating it is oxidized in the composite gas. Metals C1010 and C1018 show a moderate weight gain of 4%. Metals 310SS and alloy 800 (high Cr alloy) show no weight change. A regression analysis shows that three metals (C1018, T11, and T22) show exponential weight change in relation to time. The oxidation on the surface of metals C1018 and T11 may act as a protective coating against further corrosion. The similar experiments using composite gas without HCl were conducted at 200°C. No significant weight change was observed for all six metals (Chou et al., 1993b). The next set of laboratory corrosion experiments were carried out in composite gas containing 0.01% HCl at three temperatures (600°C, 200°C, and 100°C) for 400 hours.

All the results combined allow us to assess the effect of materials, temperature and HCl concentration on the corrosion of metals. Figure 7a and 7b show the weight loss of metals C1018 and Alloy800 at 600°C. Alloy800 is a high-Cr metal; no corrosion is observed at all HCl concentrations. In contrast, for carbon steel C1018, weight loss is observed at HCl levels of 0.01% and 0.02%. Weight gain is observed in the case of no HCl in combination gas, as a result of metal oxidation. A comparison of these two diagrams demonstrates the material effect, i.e. the high-Cr steel is more corrosion resistant because of the formation of protective thin chromia film. The results shown in Figure 7a indicate that a greater weight loss is observed when the HCl concentration in combination gas is higher.

Figure 7c, shows the results of corrosion tests on metal C1018 at 200°C. No metal corrosion is observed at this temperature at all levels of HCl concentrations. A comparison of Figures 7b and 7c shows the temperature effect; more weight loss is observed at higher temperature. Figure 7d shows the weight loss of metal C1018 at different HCl concentrations at 100°C under a moist condition. Weight loss is observed at a high HCl concentration because of the condensation of HCl on the metal surface.

Influence of calcium hydroxide on HCl concentrations in combustion gases

Coal IBC-109 was combusted in a high-temperature combustion apparatus in conjunction with a quadrupole gas analyzer (QGA). A coal sample in a ceramic boat is pushed into the combustion chamber preheated to the desired temperature (825°C or 1120°C). The combustion gases were sampled through a capillary tube and analyzed by the QGA. The intensity of ion current is proportional to the HCl concentration in the combustion gas. Figure 8 shows the results of three types of experiments: coal only without $Ca(OH)_2$, coal with 5% $Ca(OH)_2$ (Ca:S mole ratio of 2.1), and coal with 10% $Ca(OH)_2$ (Ca:S mole ratio of 4.2).

Figure 8(a) shows the sulfur evolution profiles at 1120°C. The intensity of the initial release of SO_2, which corresponds with volatilization of the coal, was lower by more than a factor of 2 in the cases with 5% and 10% $Ca(OH)_2$ added to the fuel than in the case without $Ca(OH)_2$. However, as combustion continued, much of the initially trapped sulfur was later released as shown by the profiles of SO_2 for the two samples containing 5% and 10% $Ca(OH)_2$. This was also confirmed by quantitatively trapping the SO_2 released from the combustion experiments in gas wash bottles and precipitating the sulfur as barium sulfate.

Figure 8(b) shows the QGA results of the combustion experiments conducted at 825°C. The fuel with 5% $Ca(OH)_2$ showed a reduction of SO_2 intensity by more than a factor of 3 than pure coal. Adding 10% $Ca(OH)_2$ further reduced the SO_2 content in the combustion gas. The sulfur collected in the gas wash bottles during these experiments indicated that 70 to 85% of the sulfur was captured in the ash of the coal samples containing 5 and 10% $Ca(OH)_2$ respectively. These results indicate that adding $Ca(OH)_2$ to the coal can effectively reduce the quantity of SO_2 released during combustion at temperatures near 825°C.

Figure 8(c) shows the HCl profiles for combustion tests conducted at 825°C. The QGA detected the HCl during the combustion of pure coal. When either 5% and 10% $Ca(OH)_2$ were added to the fuel, no HCl gas was detected. However, an earlier study using the same combustion apparatus showed that only a relatively small percentage (5 to 23%) of the chlorine was captured during combustion of pellets with a $Ca(OH)_2$ additive (Rapp et al., 1992). More work is needed to improve the detection of HCl by the QGA during these type of combustion experiments.

CONCLUSIONS AND RECOMMENDATIONS

1. Two techniques, pyrolysis-gas combustion-QMS and TG-FTIR and TG-IC techniques were developed for identifying sulfur and chlorine gaseous species during coal combustion. This is the first time that HCl in combustion gases is directly measured. Evolution of sulfur and chlorine gases during programmed coal pyrolysis and combustion was determined for Illinois Basin coals. Chlorine in coal is released as HCl during coal combustion. NaCl may be formed by secondary reaction.

2. Variation of sulfur species in combustion gases depends on the oxidizing condition of combustion gases (Chou et al., 1992a).

3. With various sample preparation techniques, six minerals have been unambiguously identified in a set of boiler deposit samples. Relative abundances of major minerals in boiler deposits may be estimated using the peaks listed below: mullite (2θ, 16.4°), quartz (20.85°, 50.1°), cristobalite (21.5°), anhydrite (25.5°), hematite (35.6°), feldspar (27.5-28.0°).

   Minerals in superheater and reheater deposits are mainly mullite ($3Al_2O_3 \cdot 2SiO_2$), quartz (SiO_2), cristobalite (high-temperature silica), anhydrite (calcium sulfate, $CaSO_4$), hematite (iron oxide, Fe_2O_3), feldspar, [$(Na,K)AlSi_3O_8$], sodium iron trisulfate [$Na_3Fe(SO_4)_3$] (identified in a reheater ash sample, Chou et al., 1987).Minerals in furnace wall and economizer are: magnetite (Fe_3O_4), cristobalite, hematite, plagioclase, sodium iron trisulfate (identified in a economizer sample, Chou et al., 1987).

4. SEM and petrographic examination revealed considerable details of boiler deposit formation. Molten droplets of hematite are coated with anhydrite rim, as a result of sequential melting and condensation.

5. XRF determination of 27 major, minor, and trace elements shows considerable compositional variations. Sodium and chlorine were determined by neutron activation analysis. Chlorine is highly depleted in superheater and reheater samples (<40 $\mu g/g$). Na and K are enriched in ash deposits. For instance, Na/Al ratio in the deposits is 1.5 - 3 times that in the feed coal (this work and Chou et al., 1987).

7. Metal corrosion may be caused by direct deposition

(contact) of alkali iron trisulfate, sodium chloride, or HCl on metal surfaces. If the metal is covered by a protective oxide layer, no corrosion takes place. Factors affecting superheater and reheater corrosion include: the amount of liquid sulfate on the tube, the sulfur content of coal, the chlorine and sodium contents of the coal, temperature of tube wall, and composition of the alloy (Bakker et al., 1990). However, it should be emphasized that the conditions in the laboratory tests are not identical to boilers. The data from the laboratory tests can not be extrapolated to boiler conditions. Further experiments at coal burning boilers can demonstrate the effects of chlorine on boiler corrosion. A recent EPRI report by Latham and Chamberlain (1992) is a good example of such studies.

8. Combustion experiments run at 825°C indicated that calcium hydroxide is an effective additive to reduce the SO_2 concentration in combustion gases from coal. However, at the higher temperature of 1120°C the $Ca(OH)_2$ additive was much less effective in reducing the SO_2 concentration in the combustion gases.

REFERENCES

Bakker W.T., Blough J.L., Wolowodiuk W., and Kihara S. (1990) Materials for future fossil fuel fired steam generators. Proceedings of the American Power Conference, Chicago, p. 1-9.

Chou et al. (1987) Distribution of sodium, chlorine, and sulfur in Illinois coals, removal by physical cleaning, and their behavior during combustion. Final Technical Report, September 1, 1986 through August 31, 1987 to CRSC, 24 p.

Chou C.-L. (1991) Distribution and forms of chlorine in Illinois Basin coals. In Chlorine in Coal (edited by J. Stringer and D.D. Banerjee), Coal Science and Technology 17, p. 11-29. Elsevier.

Chou C.-L., Hackley, K.C., Cao J., Donnals G.L., Ruch R.R., Pan W.-P., and Shao D. (1992b) Behavior of sulfur and chlorine in coal during combustion and boiler corrosion. Final Technical Report, September 1, 1991 through August 31, 1992, to Illinois Clean Coal Institute, Carterville, IL, 28 p.

Chou C.-L., Hackley, K.C., Cao J., Ruch R.R., Pan W.-P., and Shao D. (1992b) Behavior of sulfur and chlorine in coal during combustion and boiler corrosion. Technical Report,

September 1 through November 30, 1992, to Illinois Clean Coal Institute, Carterville, IL, 16 p.

Chou C.-L., Hackley K.C., Cao J., Frost R.R., Ruch R.R., Pan W.-P., Upchurch M.L., Cao H.B., and Shao D. (1993a) Behavior of sulfur and chlorine in coal during combustion and boiler corrosion. Technical Report, December 1, 1992 through February 28, 1993, to Illinois Clean Coal Institute, Carterville, IL, 18 p.

Chou C.-L., Hackley K.C., Cao J., Moore D.M., Xu J., Ruch R.R., Pan W.-P., Upchurch M.L., and Cao H.B. (1993b) Behavior of sulfur and chlorine in coal during combustion and boiler corrosion. Technical Report, March 1, 1993 through May 31, 1993, to Illinois Clean Coal Institute, Carterville, IL, 20 p.

Latham E.P. and Chamberlain J. (1992) Superheater corrosion in plants burning high-chlorine coals. EPRI TR-101729.

Rapp D.M., Lytle J. M., Hackley K.C., Berger R., Strickland and R., Schanche G. (1992) Carbonation as a binding mechanism for coal/calcium hydroxide pellets. Final Technical Report, Sept. 1, 1991 through Aug. 31, 1992, to Illinois Clean Coal Institute, Carterville, IL, 23 p.

ACKNOWLEDGMENTS

This work was prepared with the support, in part by grants made possible by the Illinois Department of Energy and Natural Resources through its Coal Development Board and Illinois Clean Coal Institute, and by the U.S. Department of Energy. However, any opinions, findings, conclusions, or recommendations expressed herein are those of the authors and do not necessarily reflect the views of ILENR, ICCI, and the DOE. We thank Phil Licklider of Illinois Power Co. and Richard W. DeSollar of Central Illinois Public Service Co. for samples of boiler deposits.

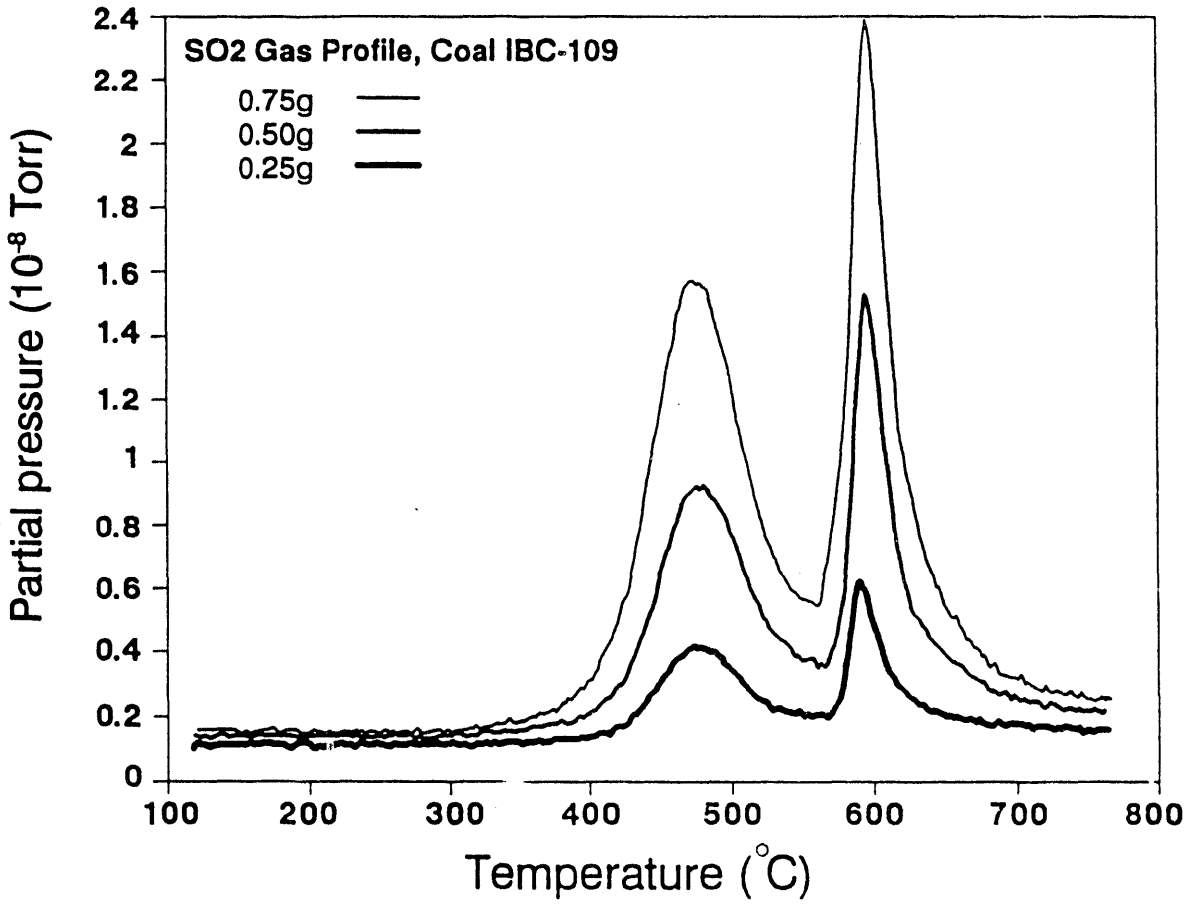

Figure 1. SO_2 evolution profiles during coal pyrolysis with three different sample weights (0.25 g, 0.50 g, and 0.75 g) of coal IBC-109. The ion current intensity is proportional to the sample weight (or the amount of sulfur).

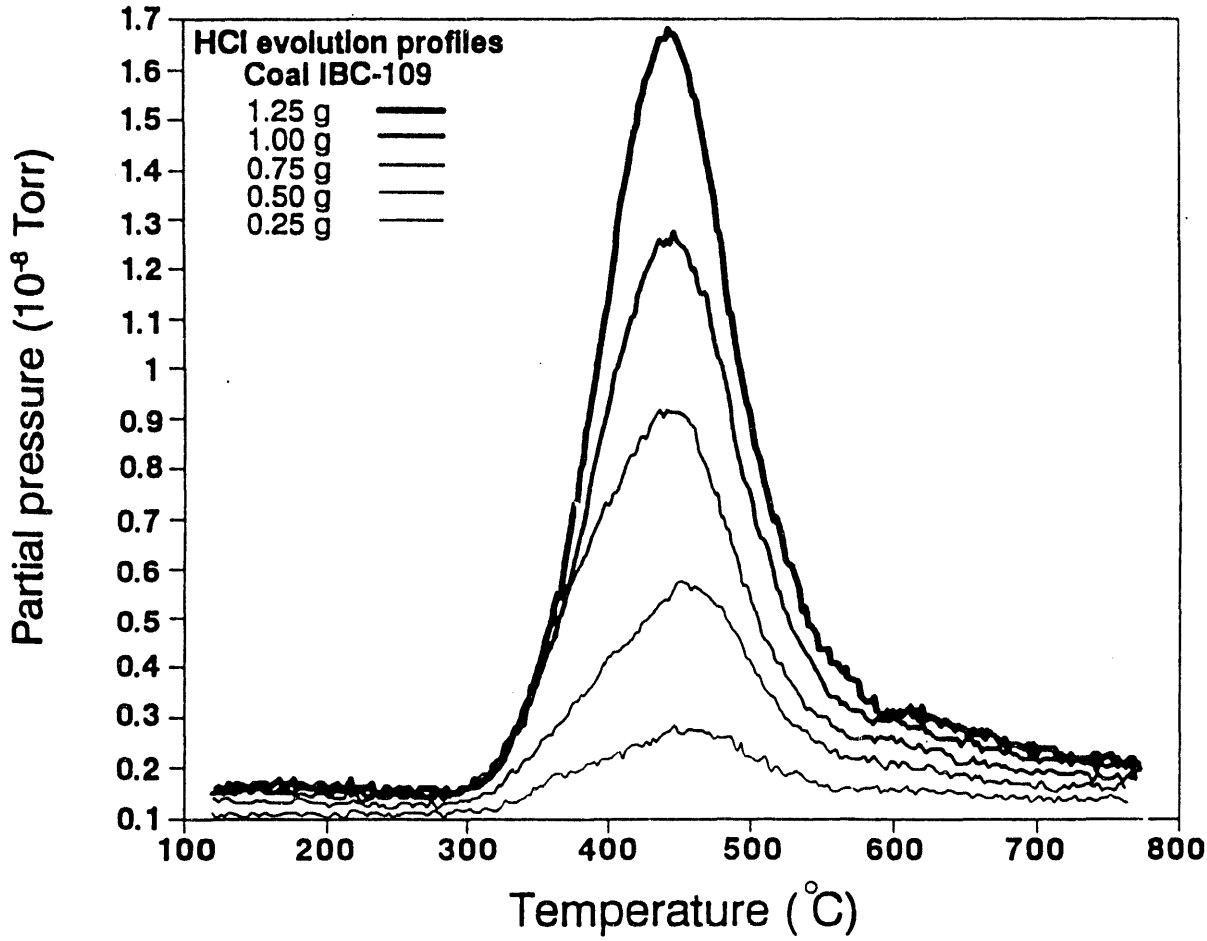

Figure 2. HCl evolution profiles during coal pyrolysis with different sample weights. Five HCl release profiles are determined by quadrupole gas analysis (mass number 36) using increasing amounts (from 0.25 g to 1.25 g) of high-chlorine coal IBC-109 (sample #109b). The HCl gas evolution from the coal begins at approximately 300°C (±10°C). The maximum rate of HCl release occurs at approximately 445°C; at 600°C the release of HCl is nearly complete. The relation between the intensity of the HCl profile and the amount of coal (hence the amount of chlorine) is clearly demonstrated.

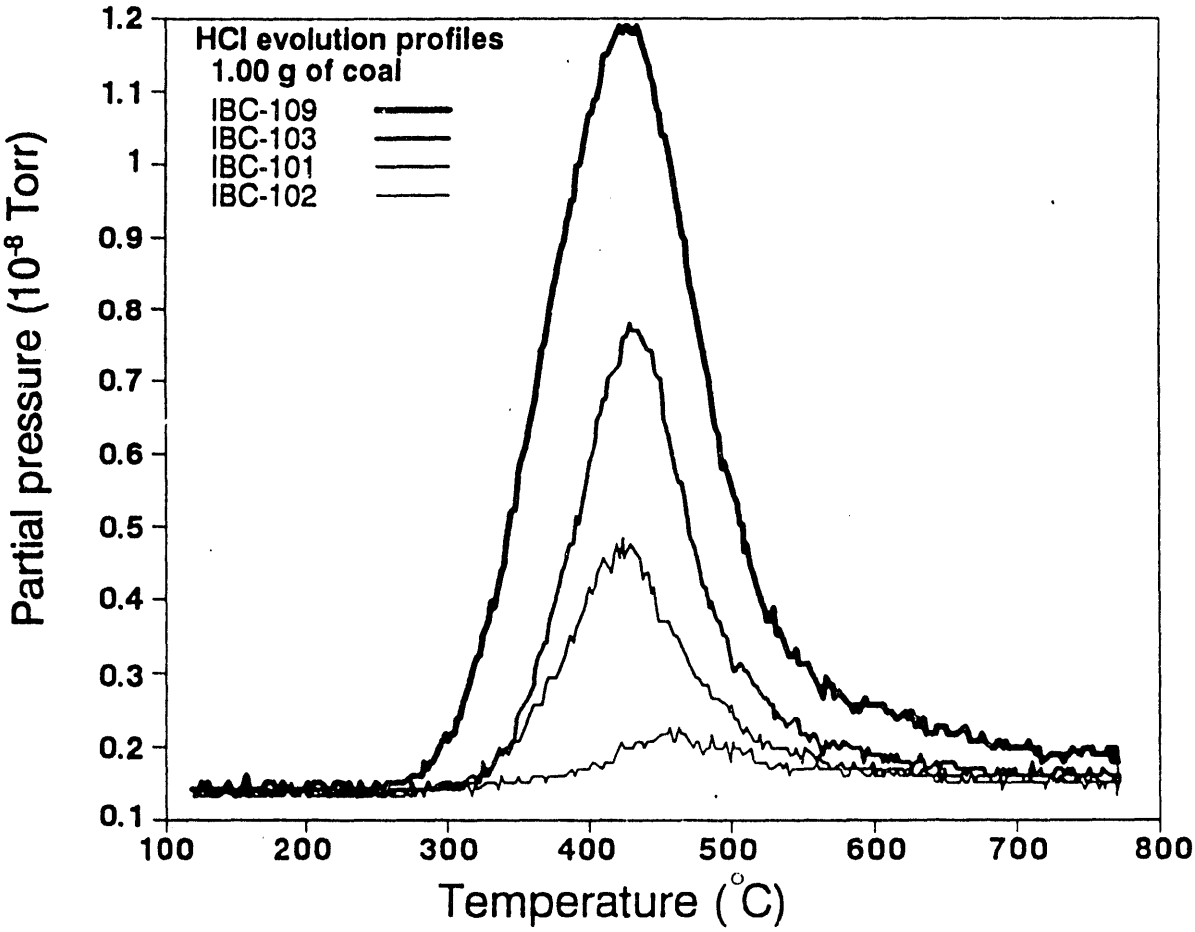

Figure 3. HCl evolution profiles of four Illinois Basin coals. Similar profiles with decreasing intensities are obtained for four coals of decreasing chlorine content from 0.42% (IBC-109), 0.18% (IBC-103), 0.10% (IBC-101), to IBC-102 (0.02%) (on dry basis). The profile for coal IBC-102 is close to the background level because of its low chlorine content.

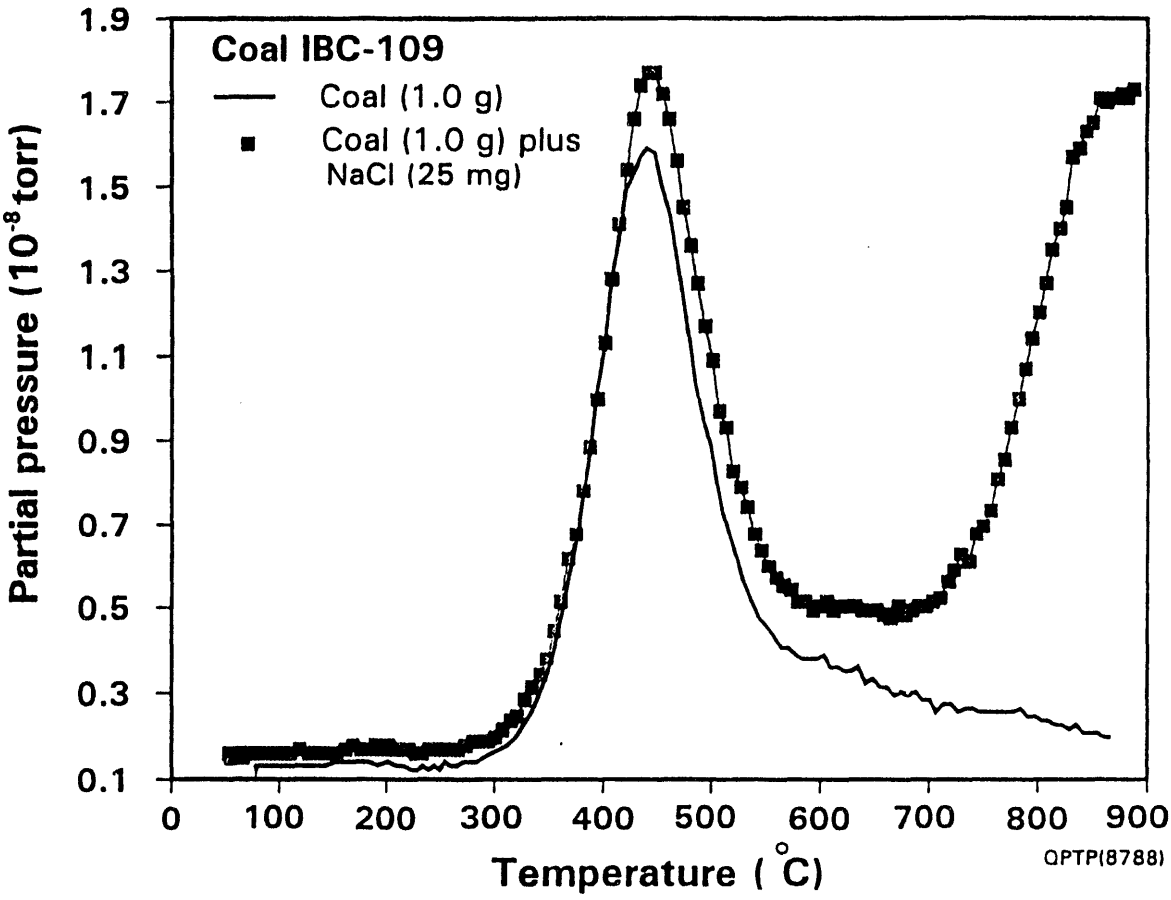

Figure 4. The release of HCl during pyrolysis of coal IBC-109 (1 g) with 25 mg NaCl in solution.

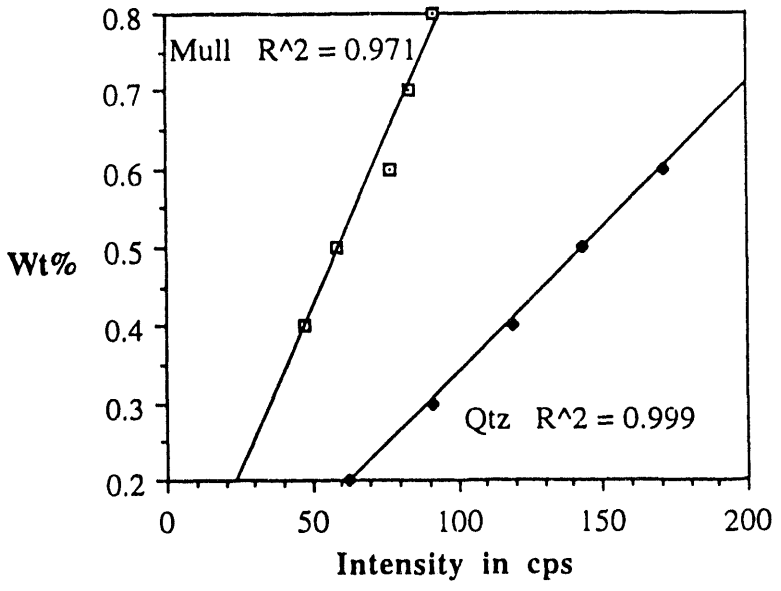

Figure 5a. Variation in intensity versus weight percent for mixtures made to establish the relation between diffraction intensity of the quartz peak at 20.85° 2θ and the mullite peak at 16.4° 2θ.

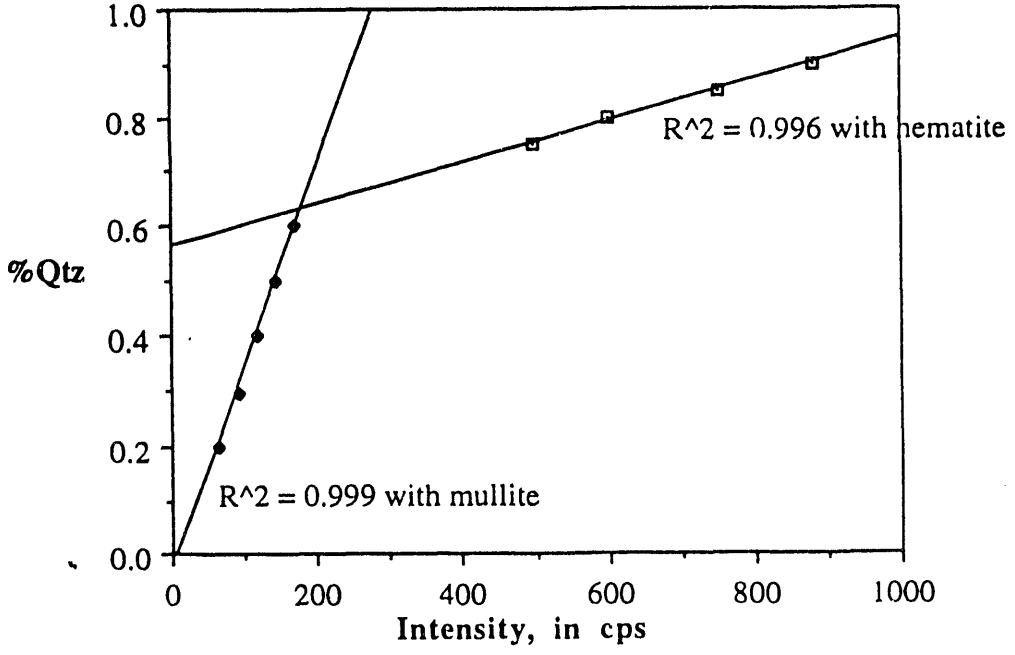

Figure 5b. Intensity responses of mullite and hematite in a quartz matrix. The difference in slopes is related to the fact that the atomic weights of the elements in mullite are similar to those of quartz, whereas the iron in hematite is heavier and absorbs more X-radiation.

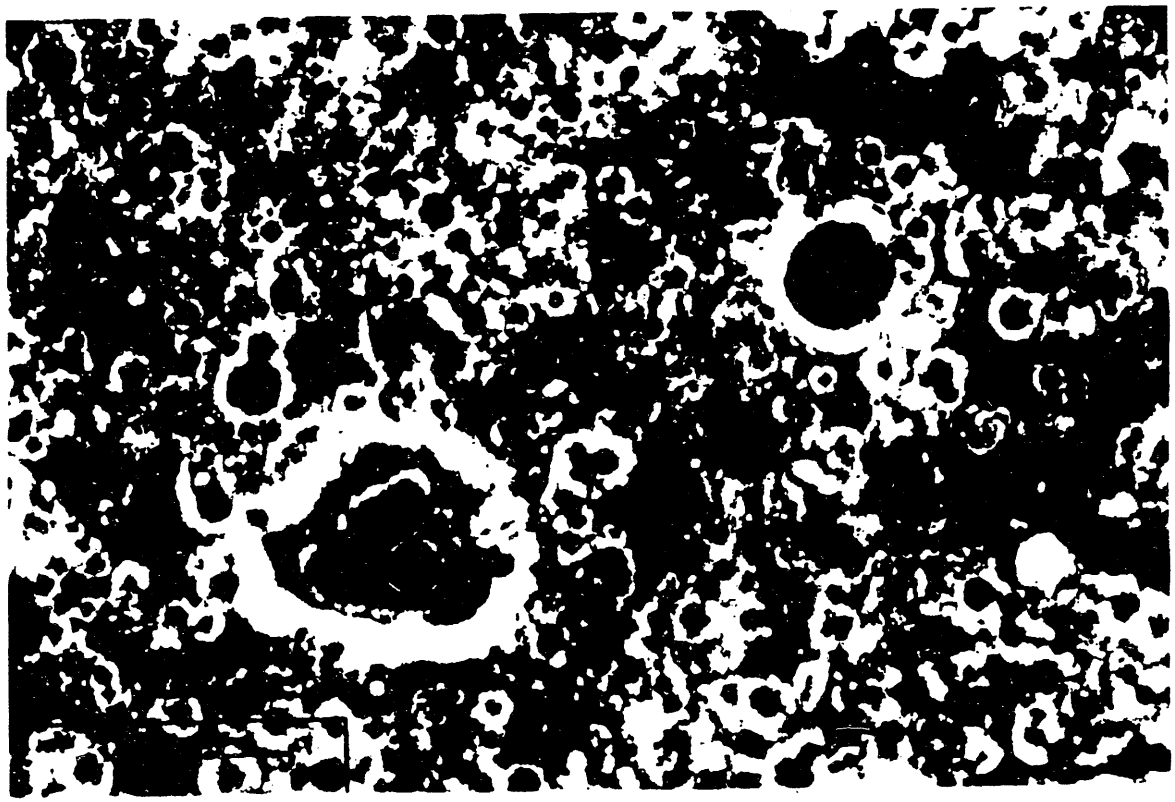

Figure 6. Petrographic view of a reheater deposit (WR5-4H) showing the occurrence of hematite and anhydrite. Hematite occurs in the form of droplets, mostly less than 50 μm in size. Anhydrite occurs in two forms, most commonly as rim coating on hematite particles. The other occurs as interstitial crystalline material. A large particle (about 200 μm) of multi-generation deposits of anhydrite and hematite lies in the lower left portion of the photo. The blue color is the space filled with epoxy. (The scale bar = 62.5 μm)

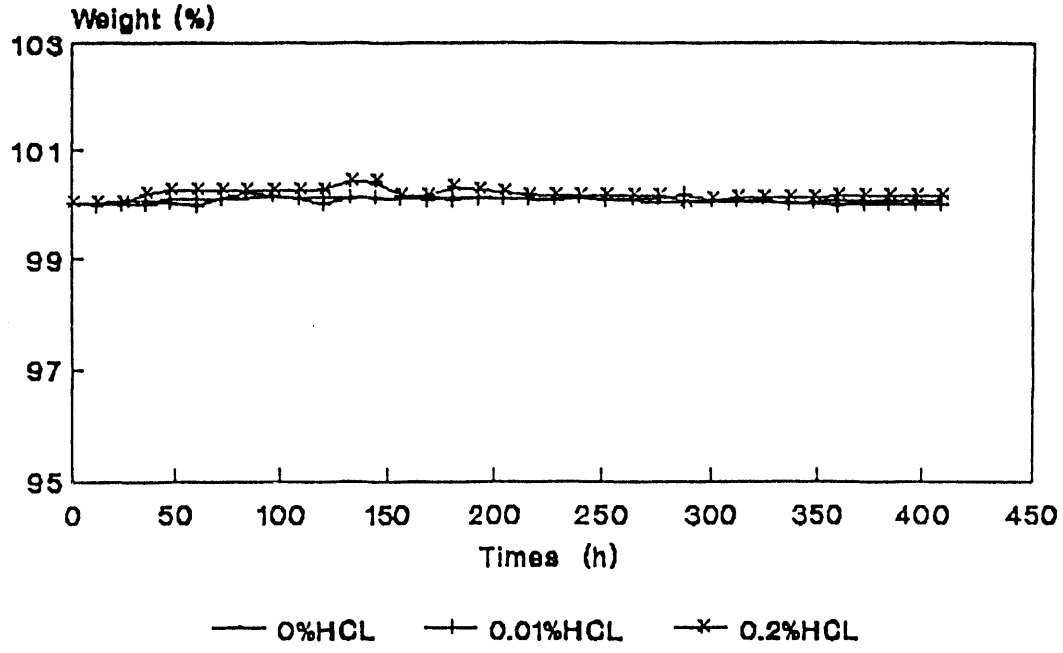

Figure 7a. Weight change of alloy800 exposed to composite gases with 0% (moist), 0.01%, and 0.2% HCl at 600°C for 400 hours.

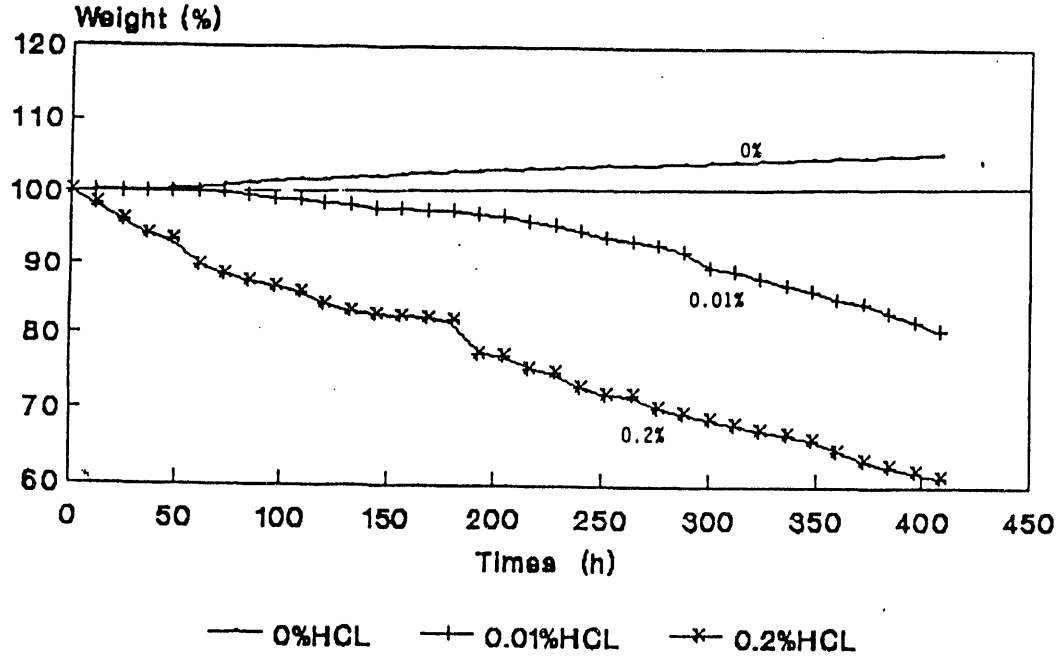

Figure 7b. Weight change of metal C1018 exposed to composite gases with 0% (moist), 0.01%, and 0.2% HCl at 600°C for 400 hours.

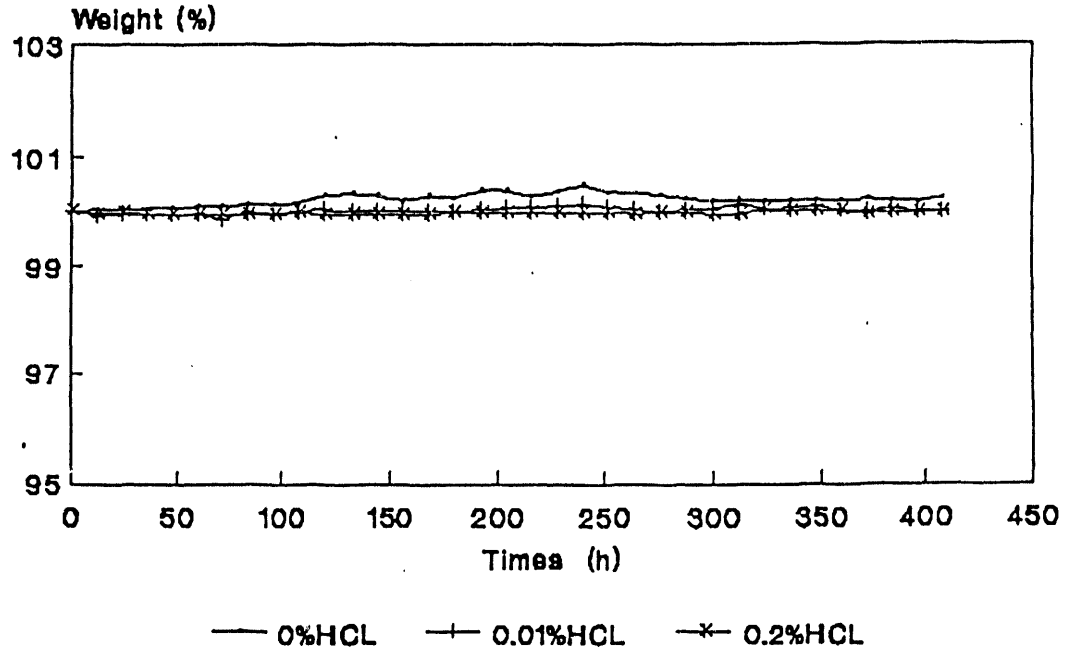

Figure 7c. Weight change of metal C1018 exposed to composite gases with 0% (moist), 0.01%, and 0.2% HCl at 200°C for 400 hours.

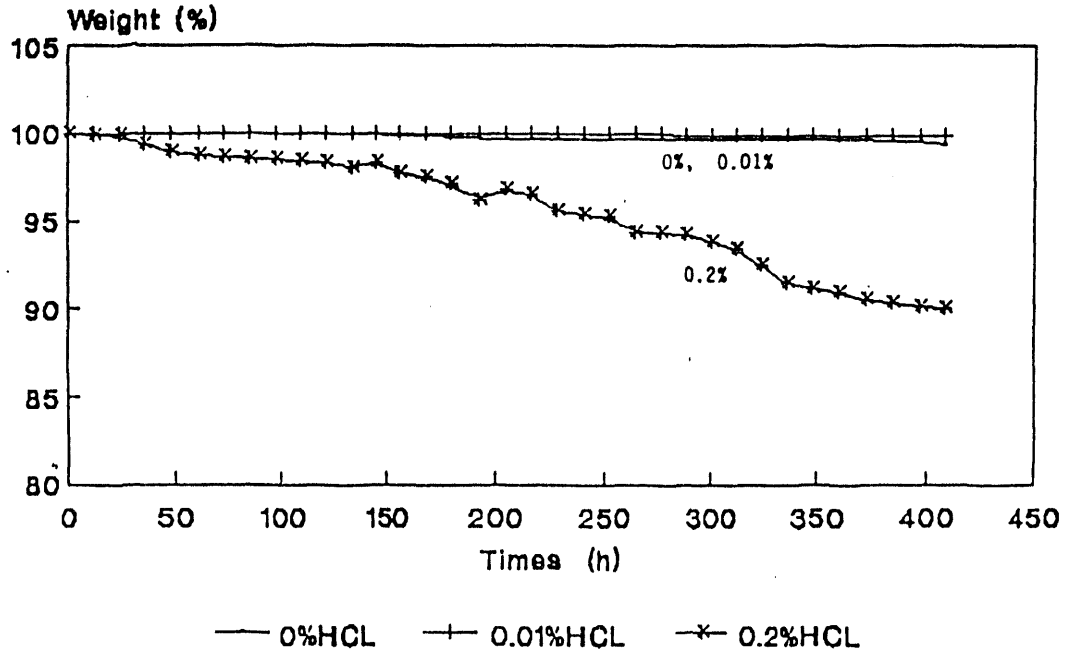

Figure 7d. Weight change of metal C1018 exposed to composite gases with 0% (moist), 0.01%, and 0.2% HCl at 100°C for 400 hours.

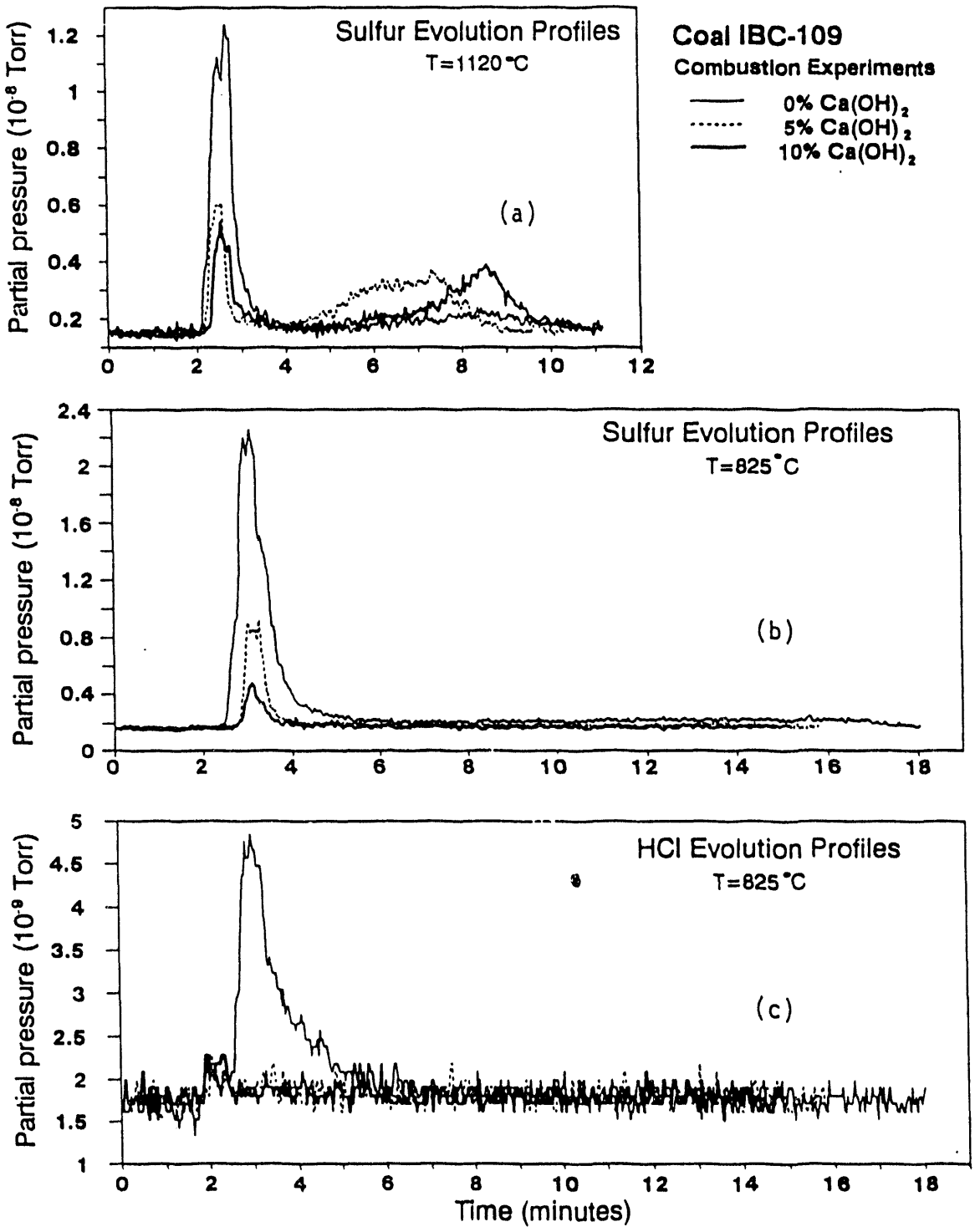

Figure 8. Influence of calcium hydroxide on the SO_2 and HCl evolution during combustion of coal IBC-109: (a) SO_2 evolution profiles at 1120°C, (b) SO_2 evolution profiles at 825°C, and (c) HCl evolution profiles at 825°C.

PROJECT MANAGEMENT REPORT
June 1, 1993 through August 31, 1993

Project Title: **BEHAVIOR OF SULFUR AND CHLORINE IN COAL DURING COMBUSTION AND BOILER CORROSION**

Principal Investigator: C.-L. Chou, Illinois State Geological Survey (ISGS)

Other Investigators: K.C. Hackley, J. Cao, D.M. Moore, J. Xu, and R.R. Ruch, ISGS; W.-P. Pan, M.L. Upchurch, and H.B. Cao, Western Kentucky University

Project Manager: K.K. Ho, Illinois Clean Coal Institute

COMMENTS

The project was successfully completed. The expenditures were consistent with the projected amounts.

EXPENDITURES - EXHIBIT B

Projected and Estimated Actual Expenditures by Quarter

Quarter (cumulative by quarter)	Types of Cost	Direct Labor	Materials and Supplies	Travel	Major Equipment	Other Direct Costs	Indirect Costs	Total
Sept. 1, 1992 to Nov. 30, 1992	Projected	4,500	600	0	0	8,000	938	14,038
	Est. Actual	4,500	320	0	0	7,938	903	13,661
Sept. 1, 1992 to Feb. 28, 1993	Projected	9,000	1,200	250	400	18,000	2,140	30,990
	Est. Actual	9,000	1,307	251	0	17,404	2,051	30,013
Sept. 1, 1992 to May 31, 1993	Projected	13,500	1,800	250	400	28,000	3,278	47,228
	Est. Actual	13,975	1,758	251	391	26,842	3,170	46,387
Sept. 1, 1992 to Aug. 31, 1993	Projected	18,344	2,400	500	400	39,753	4,650	66,047
	Est. Actual	18,655	2,576	500	344	39,322	4,650	66,047

COSTS BY QUARTER

Behavior of Sulfur and Chlorine in Coal During Combustion and Boiler Corrosion

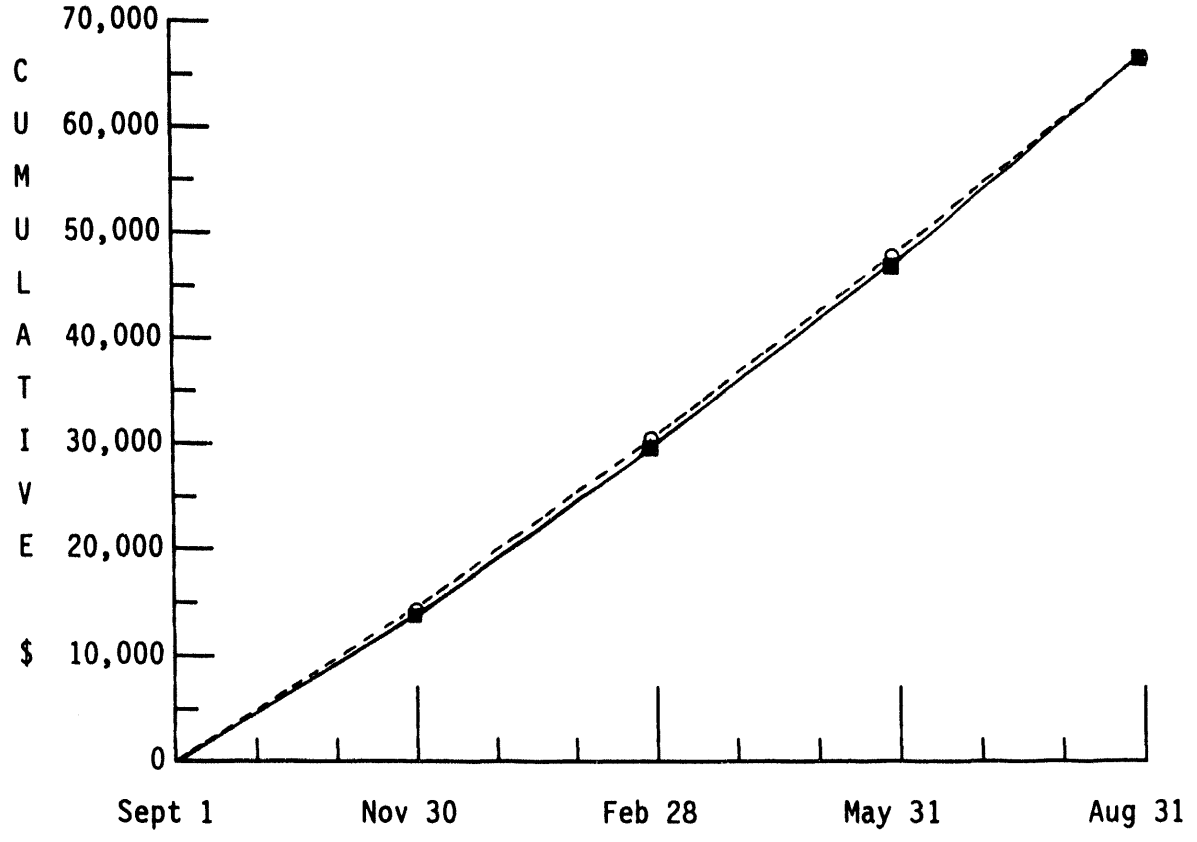

Months and Quarters

O = Projected Expenditures ----------

■ = Actual Expenditures ——————————

Total CRSC Award $ 66,047

Schedule of major milestones

September 1, 1992 - August 31, 1993

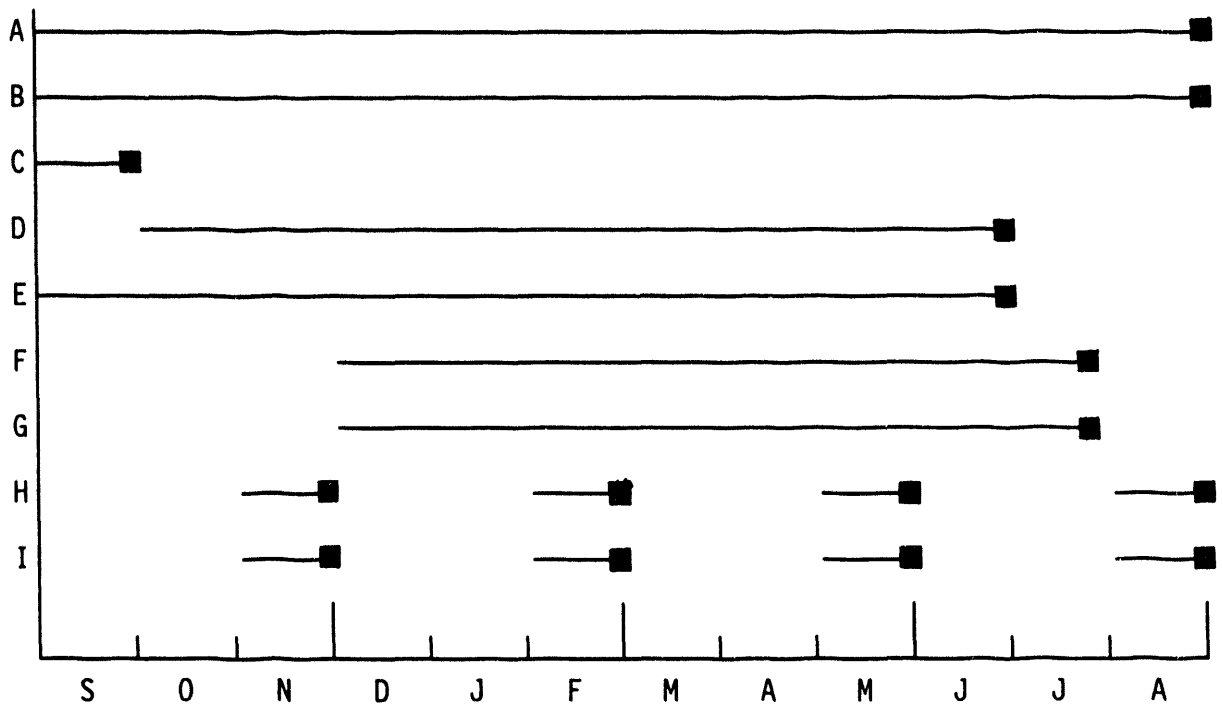

Begin
Sept. 1,1992

Milestones:

A. Employ research assistants
B. Subcontract WKU
C. Request and receive samples from utility boilers
D. Analyze boiler deposits and conduct boiler corrosion studies (Task 3, ISGS)
E. Perform laboratory corrosion experiments with simulated combustion gases (Task 4, WKU)
F. Perform combustion tests with TGA and DTA systems with FTIR spectroscopy (Task 5, WKU)
G. Perform combustion tests for coal with additives with temperature-programmed pyrolysis coupled with quadrupole gas analysis and assess remedial measures (Task 6, ISGS)
H. Prepare and submit technical reports
I. Prepare and submit project management reports

END

DATE
FILMED
4/13/94